

BEL-Float

Topic 5 – Fatigue lifetime of a FOW substructure

Deliverable 2 – Surrogate model to map fatigue strength to different EOCs

Date of delivery: 31/10/2025

Authors: ir. Victor Rappe, ir. Aico Patoor

Review: prof. dr. ing. Kris Hectors, prof. dr. ir. Wim De Waele,

University: Ghent University

Faculty: Faculty of Engineering and Architecture

Department: Department of Electromechanical, Systems and Metal Engineering

Research Group: Soete Laboratory



Financially supported by the FPS Economy (FOD Economie) under the call 2022 of the Energy Transition Fund.













Topic 5 - Fatigue lifetime of a FOW substructure Deliverable 2 - Surrogate model to map fatigue strength to different EOCs

Contents

1	Introduction 1.1 Context within BEL-Float	
2	Basics of neural networks	2
3	Surrogate model method 3.1 Data generation	3 3 6
4	Results 4.1 Feedforward neural network	9
5	Conclusion	12
\mathbf{R}_{0}	eferences	12



1 Introduction

1.1 Context within BEL-Float

This report summarises the development of surrogate models to assess the fatigue damage of welded joints of a floating offshore wind turbine (FOWT) substructure based on different environmental and operational conditions (EOCs). It represents the second deliverable (D1.1.5.3) for Topic 5 of the BEL-Float project. Where Deliverable 1 (D1.1.5.1) [1] presented a modelling strategy for the determination of local fatigue damage based on time domain metocean input, the work presented in this deliverable focuses on reducing the computational burden of detailed fatigue analyses by means of surrogate models.

1.2 Problem statement

A long-term fatigue analysis of the welded joints of a FOWT substructure requires capturing local hot spot stresses under a large number of EOCs. This can be done by extending the time domain structural load mapping and finite element (FE) stress analysis from Deliverable 1 with hot spot stress extrapolation and fatigue damage calculations. However, the cumulative computational demand of this process can be excessive when used for the thousands of load cases that must be considered for long-term fatigue analysis. Note that especially the dynamic simulations and FE analyses are the bottlenecks of this process.

Neural networks (NNs) can be used to map metocean inputs, such as wind speed and wave height, to local stress responses. This enables fatigue damage estimation caused by new, unexplored sea states without having to run the previously mentioned computationally expensive time domain simulations. I.e., the NN acts as a surrogate for both the dynamic simulation and the FE solver, as illustrated in Figure 1. The main objective of this deliverable is therefore to assess the feasibility and performance of neural network-based surrogate models in predicting the fatigue stresses at welded joints of FOWT substructures under varying EOCs.

2 Basics of neural networks

NNs are computational models organised in layers, each consisting of multiple neurons. A typical NN includes an input layer, one or more hidden layers and an output layer. the input layer receives raw data and encodes it into a format the network can process. The hidden layers transform the input data through weighted connections and activation functions, which allows the network to learn complex patterns and create more useful representations of the data, and an output layer, which produces the final result for the target variable. Neurons in adjacent layers are connected via weighted links, with each weight representing the importance of the corresponding input, and each neuron has a bias term and activation function to introduce the non-linear characteristics of the network [2]. In a feedforward neural network (FNN), information flows from the input layer through the hidden layers to the output layer. An example of an FNN with three inputs, two hidden layers and one output is illustrated in Figure 2.

The training of a NN consists of forward and backward passes. In the forward pass, the data moves through the network to generate predictions. The error between the predicted and actual values is calculated using a loss function. Examples are the mean squared error (MSE) or the mean absolute error (MAE). Through the backpropagation

Topic 5 - Fatigue lifetime of a FOW substructure Deliverable 2 - Surrogate model to map fatigue strength to different EOCs

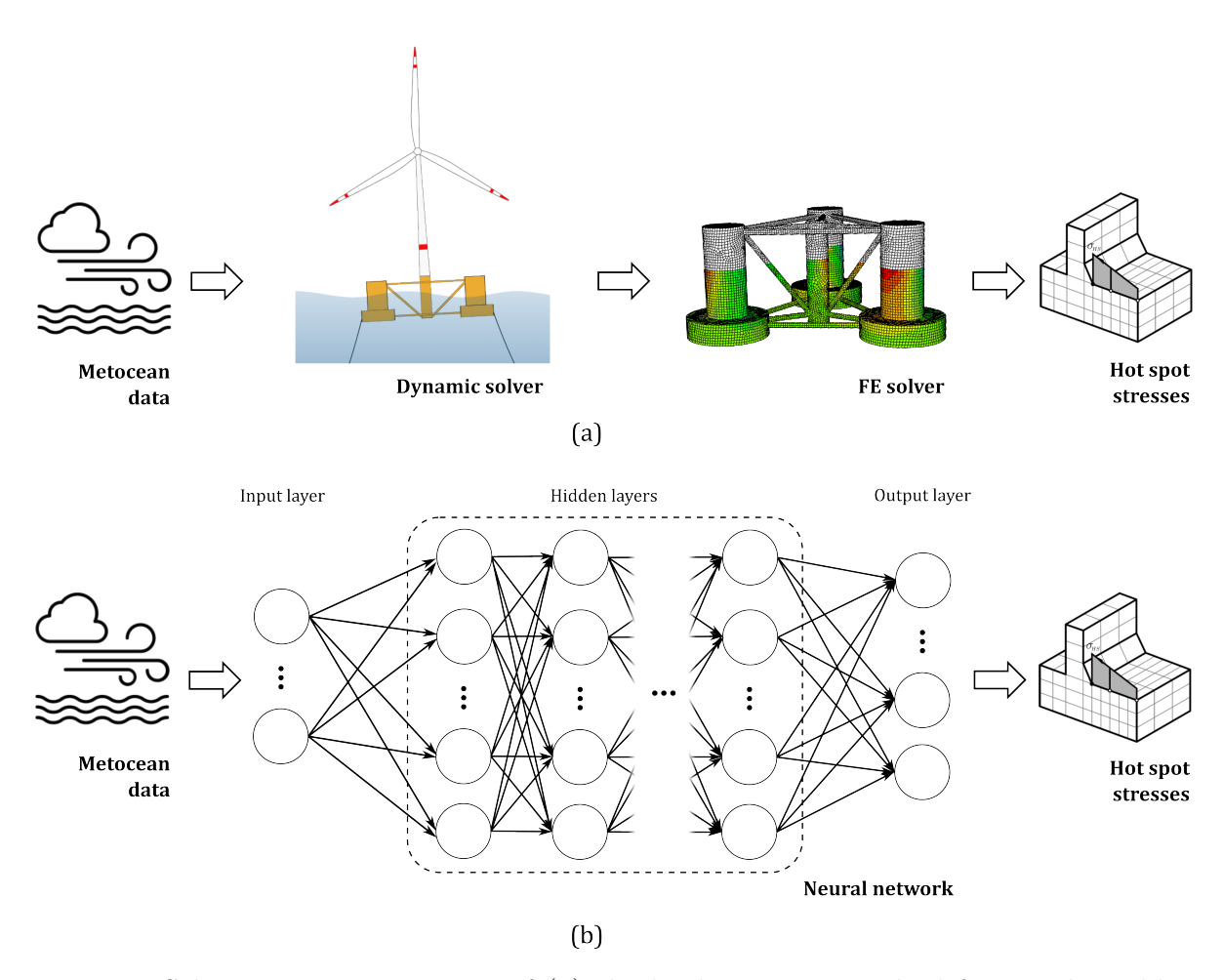


Figure 1: Schematic representation of (a) the load mapping method from Deliverable 1 and (b) the newly developed surrogate model method.

algorithm it is then computed how each weight can be adjusted to reduce the error by calculating the gradient of the loss function. An optimisation algorithm is then used to update the weights and minimize the loss.

Beyond classic FNNs, several alternative groups of architectures exist. One such group are the recurrent neural networks (RNNs), which have been specifically designed to process sequential data, such as temporal data. As illustrated in Figure 3, RNNs use a hidden state h(t) to retain information from previous timesteps, enabling the network to learn temporal patterns [3]. Long short-term memory (LSTM) and gated recurrent unit (GRU) networks are advanced variants of RNNs. LSTMs use three gates to learn temporal patterns, while GRUs use only two. For more information about the workings of (R)NNs, the reader is directed to more specialised literature.

3 Surrogate model method

3.1 Data generation

The Utsira Nord region of the coast of Norway is used for generating metocean data, as its deep waters $(185 - 280 \,\mathrm{m})$ are ideal for FOWTs and particularly for the OC4 substructure, which is typically evaluated at a depth of $200 \,\mathrm{m}$ [4]. Based on the study of Cheynet et

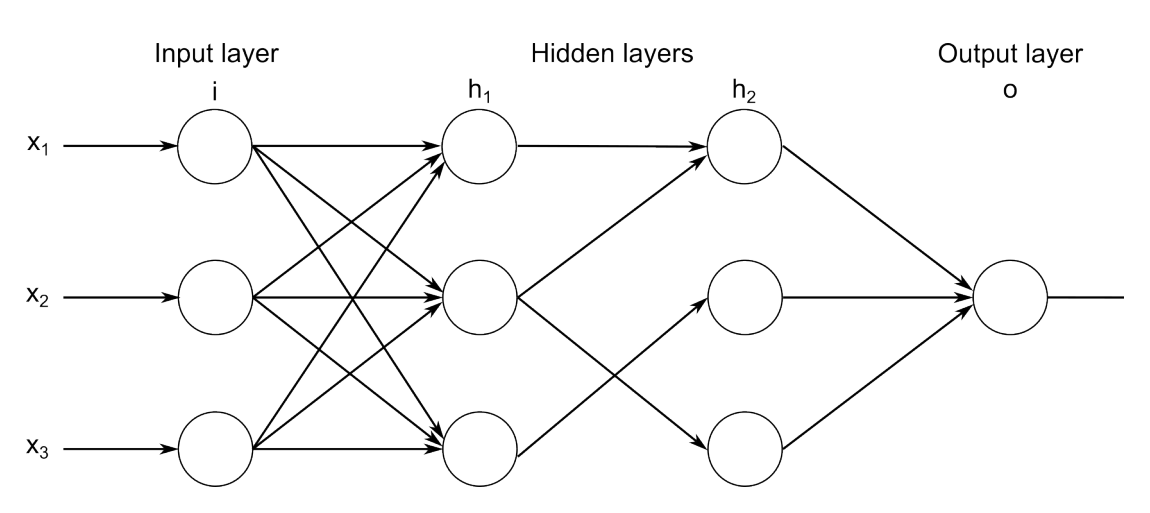


Figure 2: Example of a basic FNN with three inputs, two hidden layers and one output.

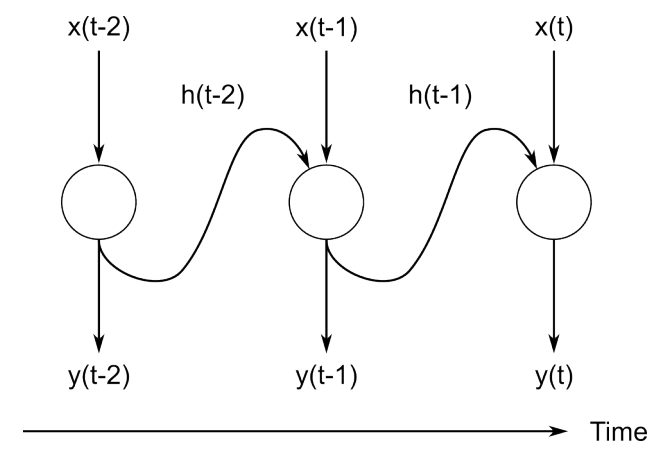


Figure 3: Example of a recurrent neuron through time. Adapted from [3].



al. [5] and the characteristics of the reference turbine, representative metocean conditions were selected, using the mean wind speed at hub height V_w , the significant wave height H_s , and the peak wave period T_p . The full combination of the selected values shown in Table 1 are considered, resulting in a total of 18 environmental states. Note that wind and waves are considered to be aligned and that the sea current is neglected. For this work, each sea state was simulated for five minutes with a temporal resolution of 0.1 seconds.

Variable	Values
Wind speed	3 m/s (cut-in), 11.4 m/s (rated), 25 m/s (cut-out)
Significant wave height	$0.5\mathrm{m},2\mathrm{m},3.5\mathrm{m}$
Peak wave period	$7\mathrm{s},12\mathrm{s}$

Table 1: Metocean variables considered for the fatigue analysis of the OC4 DeepCwind.

Using these environmental conditions, dynamic simulations were run for a stiffened version of the OC4 DeepCwind semisubmersible platform in a custom version of OpenFAST v3.5.3. The resulting time domain load series were then mapped onto a three-dimensional FE model of the substructure and solved in the linear elastic solver of Abaqus 2024. More information on the stiffened version and the load mapping can be found in Rappe et al. [6]. For this work, one critical welded region was selected for the extraction of hot spot stresses (HSS) for fatigue analysis, as shown in Figure 4. The FE model had a global element size of 750 mm, which was refined to a minimum size equal to half the thickness of the member at the weld toe for the fatigue analysis.

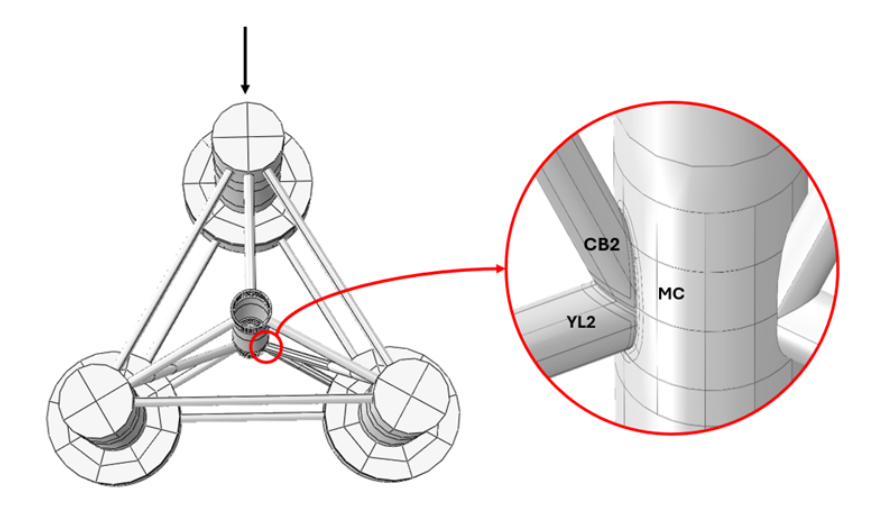


Figure 4: Illustration of the stiffened OC4 DeepCwind substructure, showing the aligned wind and wave direction with the black arrow and the considered welded region.

To calculate the fatigue life, the HSS method as defined in DNV-RP-C203 [7] was considered. For each point of interest, the stresses perpendicular to the weld toe were extracted at a distance of 0.5t and 1.5t from the weld toe, with t the thickness of the member, as illustrated in Figure 5. The HSS σ_{hs} was then calculated by linearly extrapolating the extracted stresses towards the weld toe. Note, that as the weld geometry cannot be explicitly modelled due to the use of shell elements, the intersection line of the members was used as a reference. For the considered welds, eight HSSs were extracted at



the weld toe on cross brace 2 (CB2), Y lower 2 (YL2), and the main column (MC), for a total of 24 HSS locations, as shown in Figure 6.

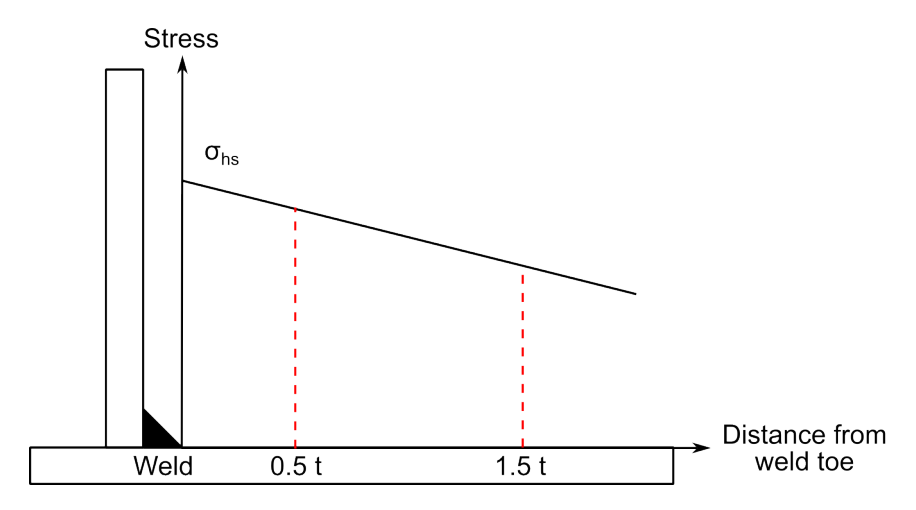


Figure 5: Hot spot stress extrapolation method as defined in DNV-RP-C203.

Finally, a database was created to train the NNs. This database contains the EOC parameters $(V_w, H_s, \text{ and } T_p)$, the time and wave elevation signals, and σ_{hs} at the 24 considered HSS locations.

3.2 Neural network architectures

All considered architectures use the EOC paramaters and time domain wave elevation signal as inputs. The output of the networks are the time domain HSSs of the 24 considered locations around the welds.

Using these inputs and outputs, three NN architectures were implemented. A FNN was used as baseline due to its simplicity and widespread use in regression tasks, and LSTM and GRU networks were used for their ability to model time dependencies. For the FNN, the dataset was randomly partitioned into a training, validations, and test set, containing respectively 80%, 10%, and 10% of the original dataset. For the LSTM and GRU, the sequential nature of the data must be respected. In these models, the first 80% of the data of each environmental state was selected as training the data, with the remainder split equally over validation and test sets.

For each type of architecture, hyperparameter optimisation was performed. This involves selecting the number of hidden layers, neurons per layer, activation functions and optimisation algorithms. Model performance was finally evaluated evaluated using MSE, MAE, and by comparing the predicted versus actual HSS time series. The hyperparameters shown in Table 2 are considered for training and evaluating the three models.

4 Results

4.1 Feedforward neural network

The FFN with the best performance consisted of one hidden layer with 128 neurons using the ReLU activation function. This model achieved the lowest MSE test loss of 0.7364 MPa². However, the difference in performance across the tested models was small, often only differing at the third decimal digit.

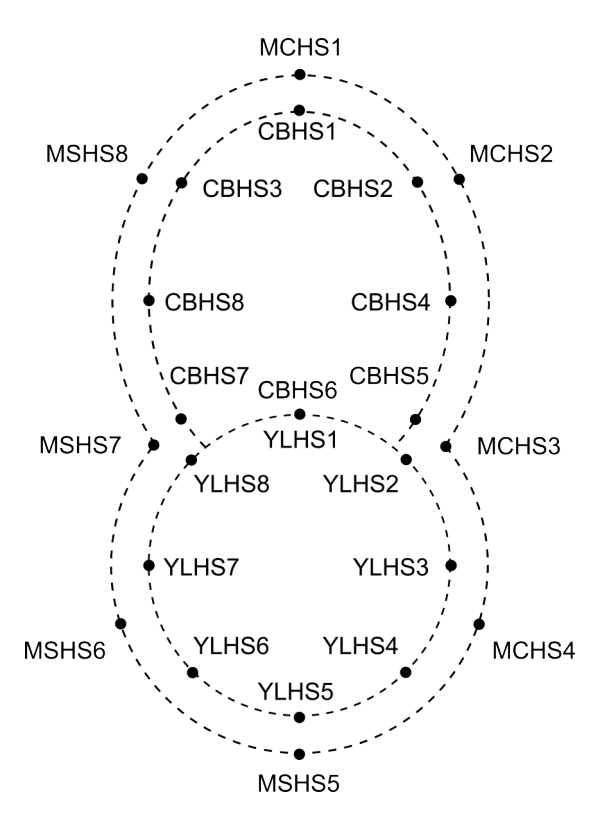


Figure 6: Locations were the hot spot stresses are evaluated for the considered welded region.

Hyperparameter	FNN	LSTM and GRU
Number of hidden layers	1, 2, 3	1, 2, 3
Number of neurons per layer	16, 32, 64, 128, 256	16, 32, 64, 128
Activation functions	ReLU, tanh, swish	tanh
Learning rate	0.001	0.001
Batch size	32, 64	32
Loss function	MSE	MSE, MAE

Table 2: Hyperparameter optimisation settings for the different architectures.



When considering the predicted versus actual HSS plot shown in Figure 7, it is observed that most of the curves are flat and centred around the y=x line. This line shows the ideal response of the network, meaning that the trained model is able to predict the mean stress, but is unable to accurately follow the time domain domain signal. This becomes more clear when considering the time domain signals illustrated in Figure 8. This figure shows the locations with the smallest (CBHS3) and largest (MCHS4) range of HSS, with their respective predicted values. It shows that the trained model predicts results around the mean stress with an almost constant amplitude, without taking the peaks and valleys into account.

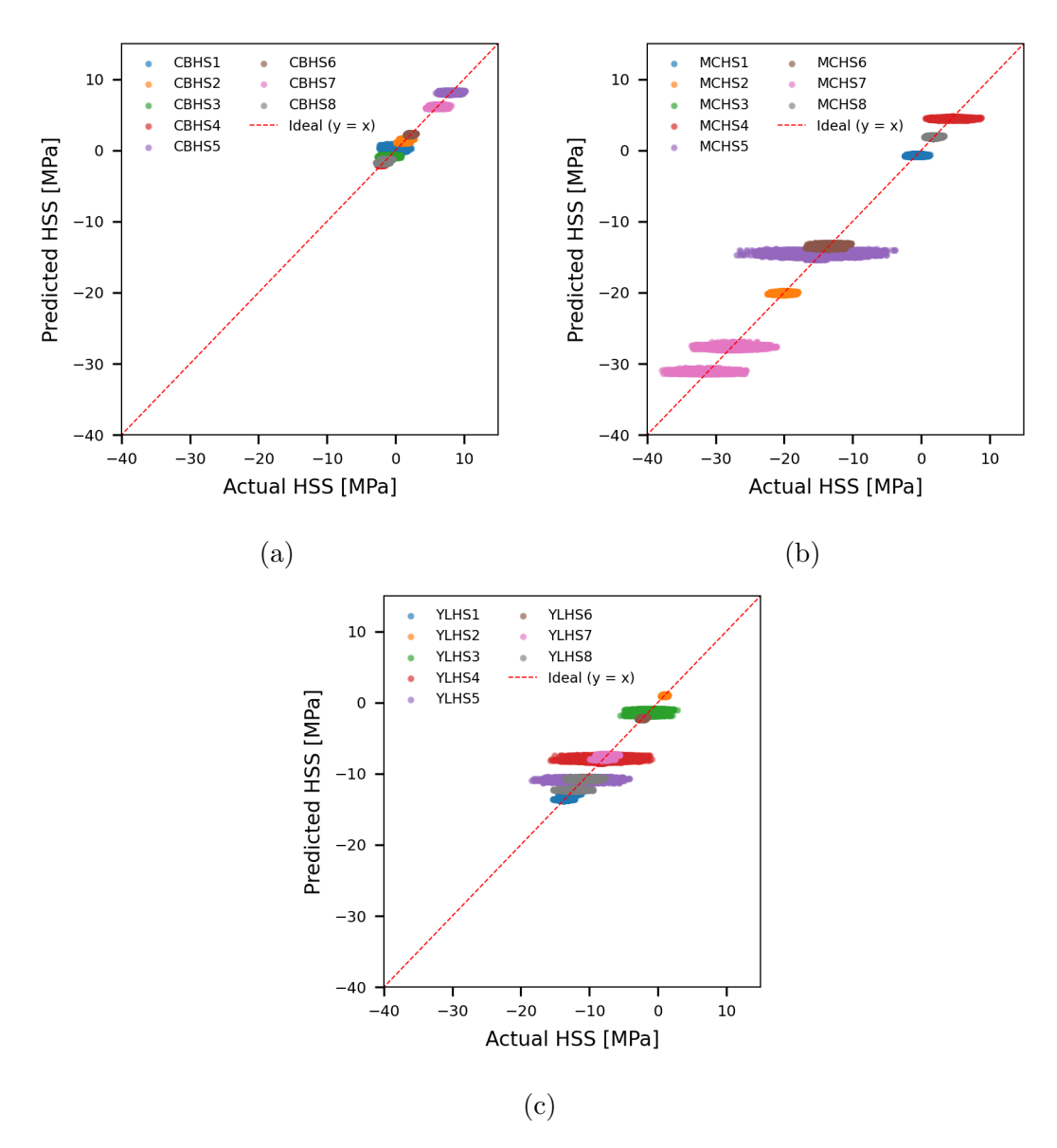


Figure 7: Predicted versus actual HSS for the points of (a) CB2, (b) MC, and (c) YL for the (128) FNN.

Surprisingly, the single layer model gave the best performance, while deeper FNNs are typically reported in literature to give better results. This is most likely due to the limited size of the currently used datasets of 18 environmental states with five minutes of simulated data for each state. As a result, the deeper models easily overfit to the data,

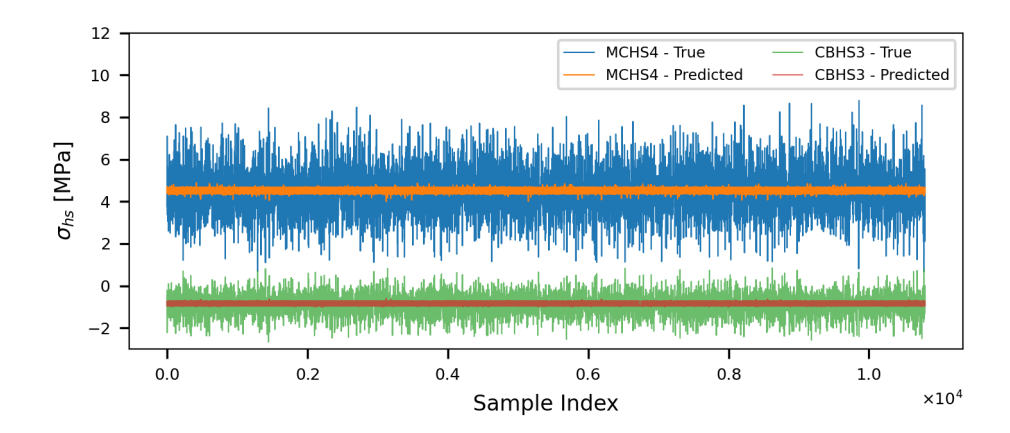


Figure 8: Comparison of the predicted and actual stress for CBHS3 and MCHS4 for the (128) FNN.

giving bad results when tested on new data.

4.2 Long short-term memory network

The LSTM model with the highest overall performance was trained using the MSE loss function and consists of two hidden layers, one with 32 and one with 16 neurons. This model achieved a test loss of 0.6318 MPa², but again the difference between the considered models was small.

When considering the predicted versus actual HSS plot shown in Figure 9, a clear difference is observed compared to the FNN model, showing more variation in the predicted stresses. Again, the trained network is able to accurately predict the mean value of the HSSs, and contrary to the mostly flat responses for the FNN, the LSTM is able to capture the dynamics more accurately. This is shown more clearly when considering the time domain test data, as illustrated in Figure 10. The trained model is able to follow the jump in mean stress between different sea states. However, it again struggles to follow the peaks and valleys of the stress response.

4.3 Gated recurrent unit network

Similar to the LSTM model, the highest performing model was trained using the MSE loss function. It consisted of a single hidden layer with 32 neurons and achieved a test loss of 0.5583 MPa², meaning that it has the best performance of the three considered architectures.

When considering the predicted versus actual HSS and the time domain signals in Figures 11 and 12, respectively, similar behaviour to the one of the LSTM network is observed. When compared to the LSTM model, the predicted versus actual HSS results are more concentrated around the y=x line, showing the better performance. However, when considering the time domain signals, the GRU is able to follow the mean HSS, but is unable to follow the peaks and valleys of the time domain signal, similar to results of the LSTM.

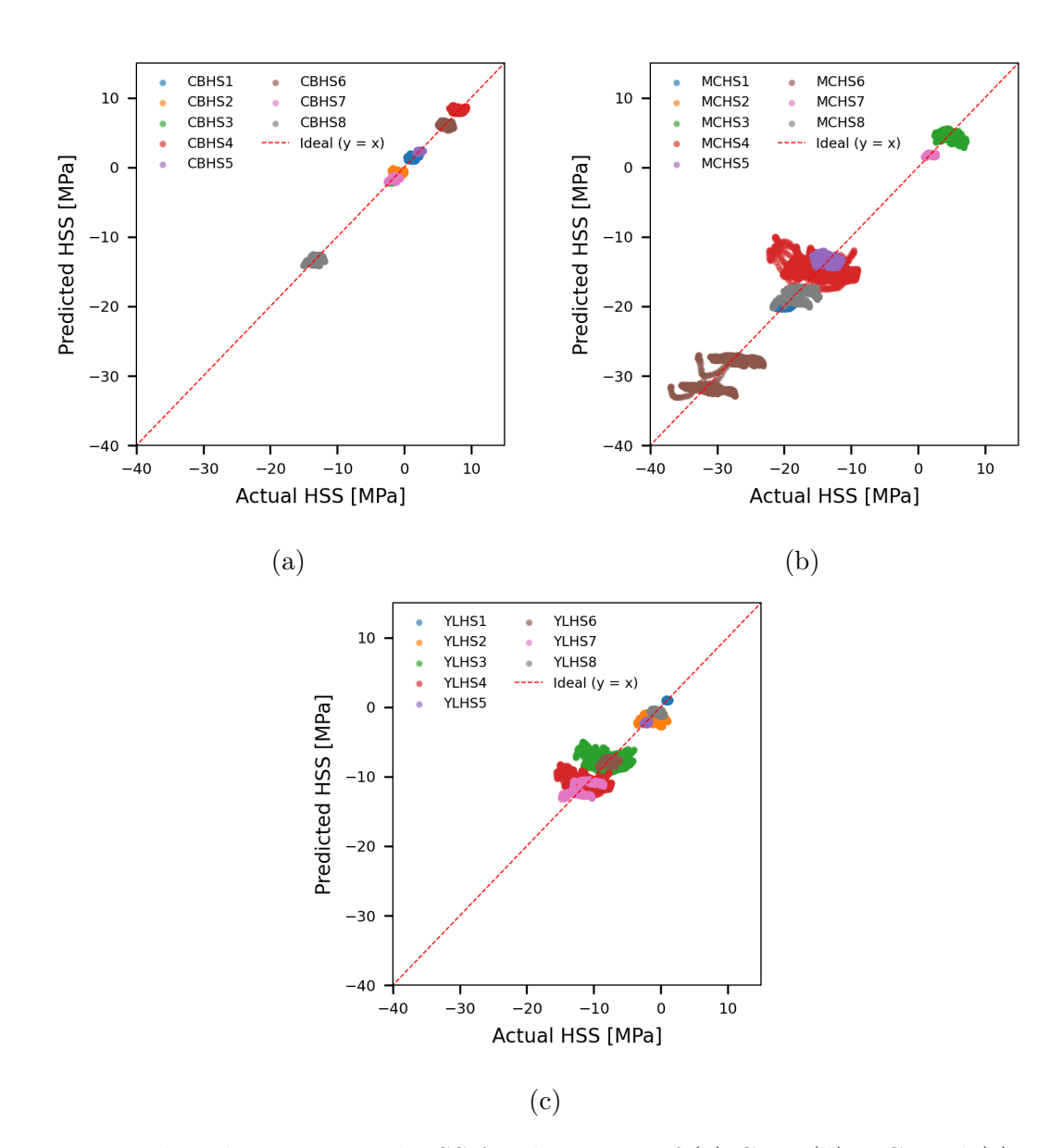


Figure 9: Predicted versus actual HSS for the points of (a) CB2, (b) MC, and (c) YL for the (32, 16) LSTM network.

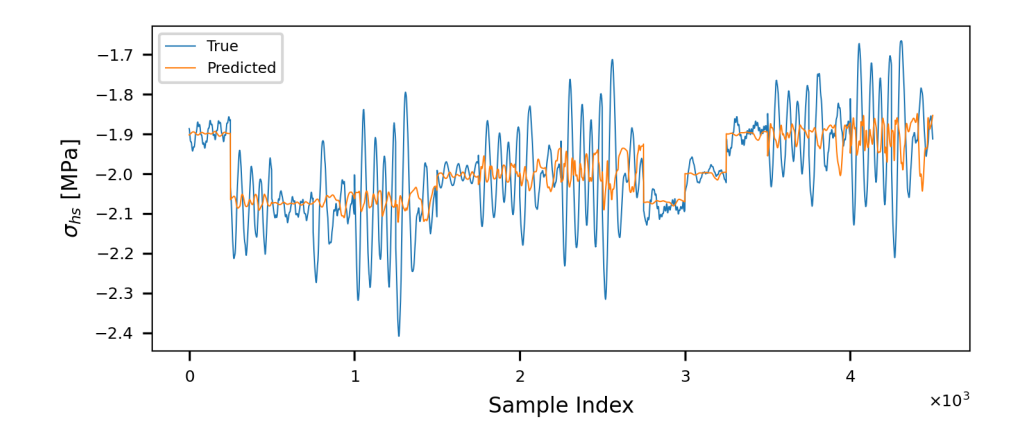


Figure 10: Comparison of the predicted and actual stress for CBHS3 for the (32, 16) LSTM network.

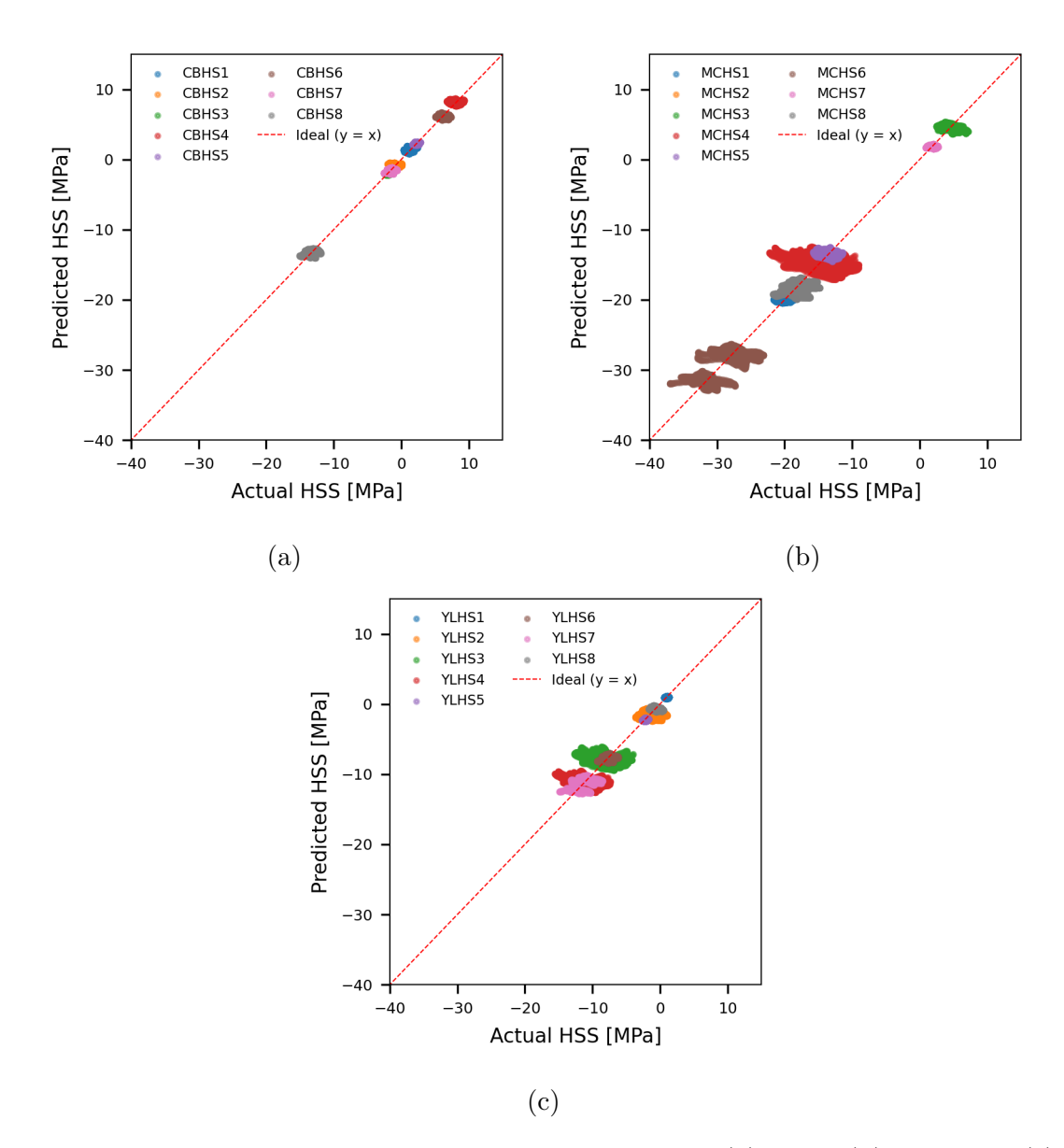


Figure 11: Predicted versus actual HSS for the points of (a) CB2, (b) MC, and (c) YL for the (32) GRU network.

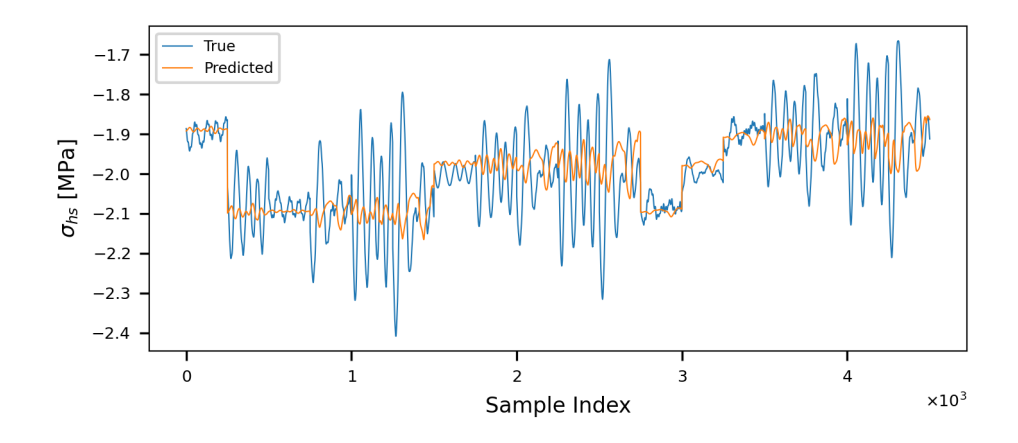


Figure 12: Comparison of the predicted and actual stress for CBHS3 for the (32) GRU network.



5 Conclusion

Among the three models, the LSTM and GRU models consistently outperformed the FNN model, showing that the time dependency of the data cannot be neglected. This is unsurprising as the dynamics of a FOWT are influenced by radiation loads, which inherently have a time dependency through the use of a convolution integral. For the RNNs, the LSTM and GRU models gave similar results, with the GRU model achieving the lowest error, showing its ability to work with limited datasets. However, even the GRU was only able to capture the mean stress response and not the peaks and valleys which are necessary for fatigue analyses.

The evaluation of the two RNN architectures shows the potential and the current limitations of surrogate models for fatigue assessment of FOWT substructures. The largest potential is that both networks are able to predict the mean HSS for all of the selected HSS points. However, while the models were all able to follow the mean stresses across different EOCs, the predicted stress amplitudes were significantly smaller than the validation data. This inability to follow the stress peaks and valleys mean that the results from rainflow-counting and subsequent application of the Palmgren-Miner rule would give extremely nonconservative results. I.e., the models do not have a good enough performance to be used for calculating the accumulation of fatigue damage and resulting lifetime.

To further improve the models, the following points will be considered. First, the time per sea state must be increased, so that a sufficient range of stochastic combinations of wind and waves are included. Second, more load cases must be considered and this must be done in a more structured method. While a long-term fatigue analysis would give unrealistic proportions to the dataset, the modified contour method [8] can be used to get a representative dataset of realistic proportions. Finally, turbulent wind and wind-wave misalignment can be considered to further improve the realism of the model.

References

- [1] V. Rappe, K. Hector, W. De Waele, Deliverable 1.1.5.1 bel-float project: Multi-dimensional modelling strategy, 2024. doi:10.5281/zenodo.15355812.
- [2] A. D. Dongare, R. R. Kharde, A. D. Kachare, Introduction to Artificial Neural Network, 2012.
- [3] J. Chen, Y. Liu, Fatigue modeling using neural networks: A comprehensive review, Fatigue & Fracture of Engineering Materials & Structures 45 (2022) 945–979. doi:10.1111/ffe.13640.
- [4] A. Robertson, J. Jonkman, M. Masciola, H. Song, A. Goupee, A. Coulling, C. Luan, Definition of the Semisubmersible Floating System for Phase II of OC4, 2014. doi:10.2172/1155123.
- [5] E. Cheynet, L. Li, Z. Jiang, Metocean conditions at two Norwegian sites for development of offshore wind farms, Renewable Energy 224 (2024) 120184. doi:10.1016/J. RENENE.2024.120184.
- [6] V. Rappe, K. Hectors, M. C. Ong, W. De Waele, An Engineering Method for Structural Analysis of Semisubmersible Floating Offshore Wind Turbine Substructures,



Topic 5 - Fatigue lifetime of a FOW substructure Deliverable 2 - Surrogate model to map fatigue strength to different EOCs

Journal of Marine Science and Engineering 13 (2025) 1630. doi:10.3390/jmse130916 30.

- [7] Det Norske Veritas, DNV-RP-C203: Fatigue design of offshore steel structures, 2020.
- [8] Q. Li, Z. Gao, T. Moan, Modified environmental contour method to determine the long-term extreme responses of a semi-submersible wind turbine, Ocean Engineering 142 (2017) 563-576. doi:10.1016/j.oceaneng.2017.07.038.